How to cite: *Angew. Chem. Int. Ed.* **2022,** *61,* e202212745
International Edition: doi.org/10.1002/anie.202212745
German Edition: doi.org/10.1002/ange.202212745

Dynamic Covalent Chemistry

Photoresponsive Dissipative Macrocycles Using Visible-Light-Switchable Azobenzenes

*Esther Nieland, Jona Voss, Andreas Mix, and Bernd M. Schmidt**

Abstract: Visible light can be used to shift dynamic covalent imine assemblies out of equilibrium. We studied a fluorinated azobenzene building block that reliably undergoes geometric isomerism upon irradiation. The building block was used in combination with two different amines, ethylenediamine and *R,R*-1,2-diaminocyclohexane, to create a library of imine macrocycles. Whereas the simple amine can be used to access a polymeric state and a defined bowl-shaped macrocycle, the chiral amine gives access to a rich network of macrocycles that undergo both isomerisation as well as interconversion between different macrocyclic species, thereby allowing for control over the number of monomers involved in the cyclo-oligomerization; ^{1}H- and ^{19}F-DOSY NMR, MALDI-MS measurements, and UV/Vis spectroscopy were used to study the processes.

Supramolecular, or dynamic covalent interactions, enable the design and synthesis of complex supramolecular systems with well-defined two- or three-dimensional architectures. They generally approach a thermodynamic equilibrium with a stable composition of supramolecular structures.[1] As this dynamic covalent chemistry (DCC) allows for error correction during the formation of said supramolecular entities, the yields and selectivities are often high.[1f] The self-assembled structures can have a variety of different exciting properties, and the reversible formation of metal-free systems using boronate esters, imines, and alkynes is very well established.[1c,d] Enabling these systems to become stimulus responsive can allow for the controlled assembly or disassembly of systems, or can induce geometry changes and trigger guest release, adding an additional layer of information.[2] For remote-control, light has a high temporal and spatial resolution, is cheap, and generates no waste, in contrast to chemical fuels.[3] Azobenzenes, as one of the most commonly used photoswitches, bear several advantages, such as a distinct geometry change upon isomerisation, minimal photodegradation, and, in some cases, the ability to switch with visible light.[3] Creating bridged azobenzene derivatives[4] or implementing electron-withdrawing substituents such as, for example, fluorine,[5] chlorine,[6b] or electron-rich methoxy[6a,c] in *ortho*-position enables visible light switching and further improves photochemical properties. Replacing one or both benzenes in azobenzene with a heteroaromatic ring also alters the photochemistry, leading to long thermal half-lives and improved photoswitching.[7] The incorporation of azobenzenes into different supramolecular structures was utilised to generate, among others,[2b,8] metal organic cages with switchable interior hydrophobicity[8g] and photoresponsive porous liquids.[8a] Photoswitches can also be used to synthesise photoresponsive metal organic structures[9] that can undergo dissipative reactions, as recently shown by the groups of Clever,[9a] and Beves.[9b] In dissipative systems, a precursor is activated, for example by converting a chemical fuel to waste[10a] or by light,[10b–e] and undergoes reversible assembly. This process competes with a deactivation process, which can be either triggered by an external stimulus, such as chemical fuel, light, or heat, or the system spontaneously disassembles to recover the precursor.[11] The dissipative assembly or interconversion of imine systems, in contrast, has been mostly obtained by adding a fuel or a metastable acid until now.[12]

We present the formation of different dissipative or metastable dynamic covalent systems using photons as a stimulus, allowing control over the number of monomers involved in cyclo-oligomerization that leads to ring contraction and extension. The *ortho*-fluorinated, red light switchable 4,4′-(diazene-1,2-diyl)bis(3,5-difluorobenzaldehyde) (**A**), which was first synthesised by the group of Pianowski,[5a] was used in combination with two different amines, ethylenediamine (**E**) and *R,R*-1,2-diaminocyclohexane (**D**) to create a library of imine macrocycles. Combining the more stable azobenzene isomer *E*-**A** and **E**, an insoluble polymer is formed in higher concentrations, while the reaction of the less stable *Z*-azobenzene leads to the selective formation of a *Z,Z*-$\mathbf{A^2E^2}$[13] macrocycle. In contrast, $\mathbf{A^3D^3}$ was formed as the major product when using *E*-**A** with **D**, while using a *Z*-**A** enriched reaction mixture leads to the formation of several macrocycles. Intriguingly, the dissipative transformation of the macrocycle $\mathbf{A^3D^3}$ to a mixture of

[*] E. Nieland, J. Voss, Dr. B. M. Schmidt
Institut für Organische Chemie und Makromolekulare Chemie, Heinrich-Heine-Universität Düsseldorf
Universitätsstraße 1, 40225 Düsseldorf (Germany)
E-mail: Bernd.Schmidt@hhu.de
Dr. A. Mix
Institut für Anorganische Chemie und Strukturchemie, Universität Bielefeld
Universitätsstr. 25, 33615 Bielefeld (Germany)

different sized macrocycles can be achieved by irradiation with red light.

Azobenzene **A** shows a high thermal half-life, can be switched with visible light, and has a high ratio of *Z*-azobenzene in the photostationary state (PSS). Because **A** undergoes a significant geometry change when switched, we predicted that by combining *E*- and *Z*-**A** with different diamines, we would be able to access different dynamic covalent entities in solution. Building block **E** encodes little to no precoordination, so the resulting imine should be mostly governed by the structure of the azobenzene isomer employed. As expected, the reaction of **E** and *E*-**A** only led to the formation of insoluble red oligomers (see Supporting Information, page S13). In contrast, *Z*-**A** and **E** selectively formed the small *Z,Z*-$\mathbf{A^2E^2}$ macrocycle after 19 hours at room temperature under continuous irradiation with red light (660 nm) (Figure 1). The formation was observed by ^{1}H- and ^{19}F{^{1}H} NMR and MALDI-MS. Single-crystal X-ray analysis of *Z,Z*-$\mathbf{A^2E^2}$ reveals a bowl-like structure in which both azobenzenes are pointing upwards with the amine units pointing downwards (Figure 1c). In low concentrations (6.98 μM) the azobenzenes in *Z,Z*-$\mathbf{A^2E^2}$ can be isomerised from *Z* to *E* using UV (405 nm) or blue (470 nm) light, and *vice versa*, using red (660 nm) or green (565 nm) light (see Supporting Information, Figures S43–S46). In higher concentrations (2.67 mM), irradiation with UV light leads to the immediate formation of a red precipitate that consists most likely of $\mathbf{A''E''}$ oligomers (see Supporting Information, Figure S63).

Diamine **D** was chosen for its intrinsic precoordination known to reliably give access to trianglimines,[1e] which in combination with *E*-**A** selectively leads to the formation of *E,E,E*-$\mathbf{A^3D^3}$. ^{1}H- and ^{19}F-DOSY NMR spectra were recorded and show that the macrocycle has a solvodynamic radius of between 7.81 and 8.29 Å (see Supporting Information, Figures S22 and S24). Irradiating a solution of **A** with red light (660 nm) until the PSS was reached prior to the addition of **D**, led to a mixture of different macrocycles as confirmed by NMR and MALDI-MS, and the formation under continuous irradiation with red light was monitored over several days (Figure 2 and Supporting Information, Figures S13–S15). After the system reached equilibrium (after 151 hours), the solution was stirred in the dark for 112 hours, during which monitoring by NMR and MALDI-MS was continued. To assign the signals to the species, ^{19}F-DOSY NMR spectra were recorded, confirming the formation of macrocycles of different sizes. The signal with the largest intensity at −119.68 ppm after 19 hours can be assigned to an $\mathbf{A^2D^2}$ macrocycle, as the ^{19}F-DOSY shows a diffusion coefficient for this signal corresponding to a solvodynamic radius of 5.93 Å. Surprisingly, this signal broadens and shifts upfield until it merges with the signal at −119.84 ppm during the irradiation with red light and the following period in the dark. As the new signal has a similar solvodynamic radius of 6.02 Å, it can be assumed that apparently two types of *Z,Z*-$\mathbf{A^2D^2}$ are formed. The peak gradually increases in intensity but declines when the irradiation is stopped. At the start of the irradiation, another species is formed, as seen by the ^{19}F{^{1}H} NMR peak at

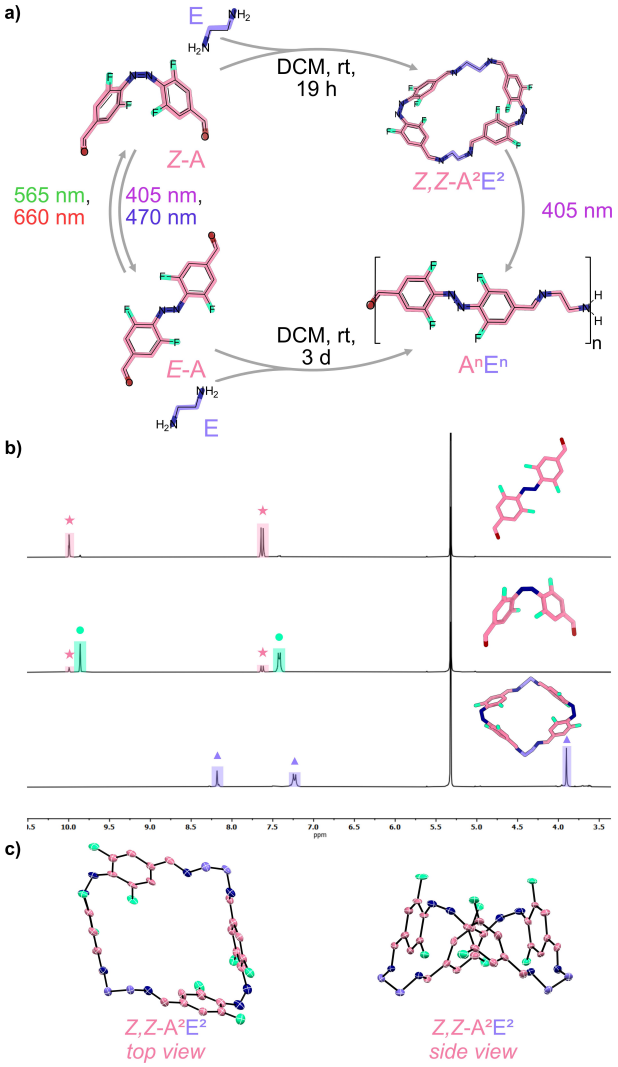

Figure 1. a) Reaction of both azobenzene isomers *Z*-**A** and *E*-**A** with diamine **E** to yield the macrocycle *Z,Z*-$\mathbf{A^2E^2}$ and the oligomer $\mathbf{A''E''}$, respectively, with geometries obtained from force field calculations; b) ^{19}F{^{1}H} NMR spectra showing the *E* (pink star) to *Z* (turquoise circle) isomerisation of **A**, followed by the formation of *Z,Z*-$\mathbf{A^2E^2}$ (blue triangle) (CD_2Cl_2, 282 MHz); c) molecular structure of *Z,Z*-$\mathbf{A^2E^2}$ as seen from the top and from the side as determined by single-crystal X-ray diffraction measurement[14] (thermal ellipsoid representation with 50% probability ellipsoids); hydrogen atoms and solvent molecules are omitted for clarity (see Supporting Information, Figures S47–S48).

−120.67 ppm, which can be assigned to an $\mathbf{A^3D^3}$ macrocycle, according to its solvodynamic radius of 6.98 Å. After 2 days, a signal can be observed which has the same chemical shift as the *E,E,E*-$\mathbf{A^3D^3}$ macrocycle (−120.36 ppm). The increasing intensity during the irradiation and in the dark can be attributed to the thermal back isomerisation of the azobenzenes in the $\mathbf{A^2D^2}$ macrocycles and the concomitant decay to the most favoured product starting from *E*-**A**, $\mathbf{A^3D^3}$. These results are supported by MALDI-MS measurements, which confirm the formation of $\mathbf{A^2D^2}$ as the major product at the start of the irradiation, alongside $\mathbf{A^3D^3}$ and $\mathbf{A^4D^4}$. The latter seems to be formed in minor quantities, as the $\mathbf{A^4D^4}$ species cannot be observed in the NMR-spectra. In relation to the

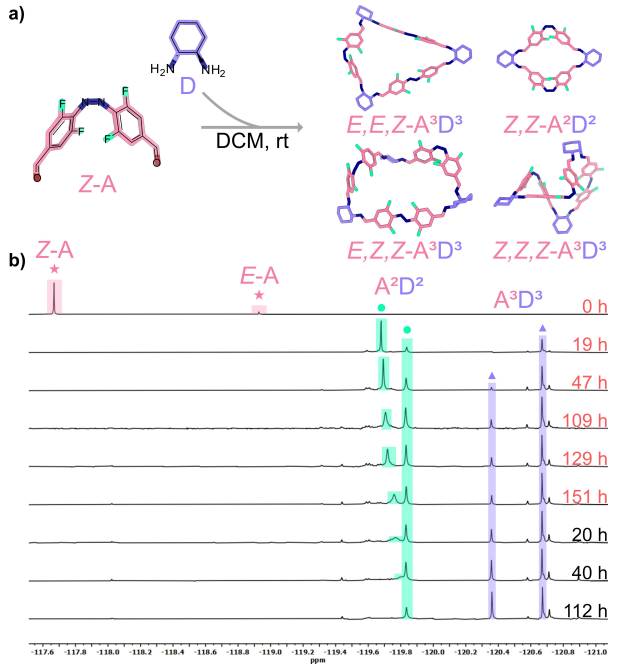

Figure 2. a) Reaction of *Z*-**A** and diamine **D** to yield different macrocycles, with geometries obtained from force field calculations; b) ^{19}F-{^{1}H} NMR spectra showing macrocycle assembly under continuous irradiation with red light (times highlighted in red) and in the dark (highlighted in black) (CD_2Cl_2, 282 MHz). The azobenzene isomers are highlighted in pink (star), the **A²D²** macrocycles in turquoise (circle), and the **A³D³** species in blue (triangle), with geometries obtained from force field calculations.

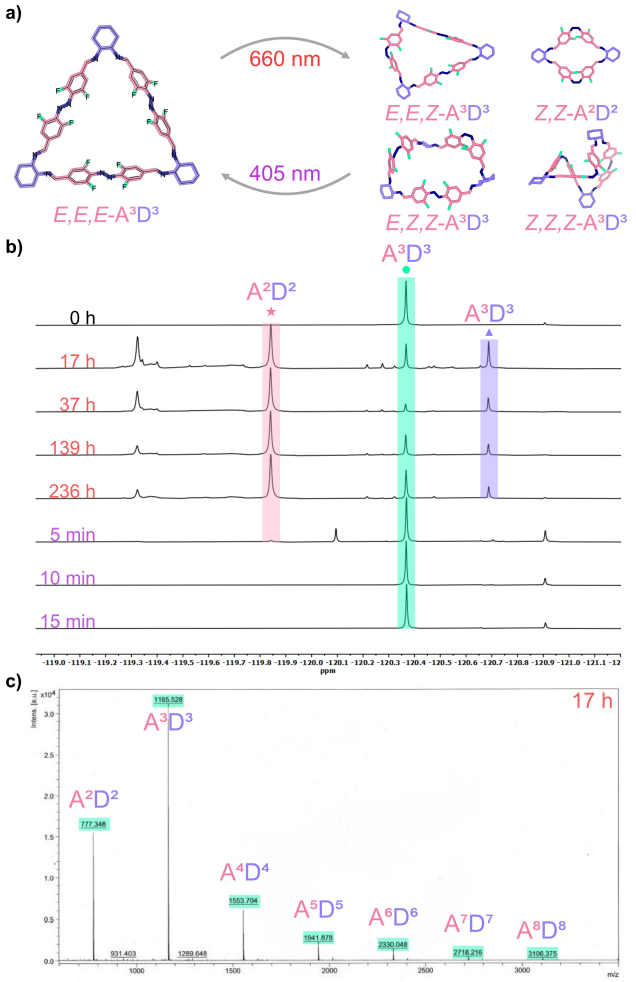

Figure 3. a) Irradiation of **A³D³** with red light (660 nm) leads to the formation of different-sized macrocycles, with geometries obtained from force field calculations. The precursor can be regained by irradiation with UV light (405 nm); b) ^{19}F{^{1}H} NMR spectra showing the transformation of **A³D³** under irradiation with red light (highlighted in red) and UV light (highlighted in violet) (CD_2Cl_2, 282 MHz) with the **A²D²** species highlighted in pink (star), **A³D³** species in turquoise (circle) and blue (triangle); c) MALDI-mass spectrum of the reaction mixture after 17 hours of irradiation with red light (660 nm).

peaks for the larger sized macrocycles, the **A²D²** peak decreases significantly once and the longer the solution is kept in the absence of light.

To verify that the photochemical properties of **A** undergo no major change upon imine formation and to get further insight into our dynamic systems, a model compound (**AC²**) was synthesised starting from **A** and cyclohexylamine (**C**). While the comparison of the UV/Vis spectra of **A** and **AC²** shows a bathochromic shift for the π→π* band (314 nm to 340 nm) upon imine formation, the n→π* band remains unchanged (475 nm). As a result, the imine compounds can also be photoisomerised with green and red light (see Supporting Information, Figures S33–35) with high ratios of *Z* in the PSS (see Supporting Information, Figures S1–S12, Tables S1–S2). The formation of **AC²** was also observed closely by NMR to get a detailed insight into the kinetics of the imine formation, confirming that the reactivity of the aldehyde undergoes no significant change upon isomerisation (see Supporting Information, Figures S49–S60). Next, we investigated the photoswitching and the dissipative reaction of **A³D³**. In UV/Vis concentrations (3.45–5.92 μM), **A³D³** undergoes *E* to *Z* isomerisation under irradiation with red (660 nm) or green (565 nm) light (see Supporting Information, Figure S36). In higher concentrations, a dissipative reaction takes place, yielding smaller **A²D²** and isomerised **A³D³** macrocycles, as confirmed by ^{1}H- and ^{19}F{^{1}H} NMR, as well as ^{19}F-DOSY NMR (see Figure 3 and Supporting Information, Figures S16–S18, S24–S26). In contrast to the formation of the macrocycle mixture when employing *Z*-**A**, only one species of an **A²D²** macrocycle is initially formed (−119.84 ppm, r_s = 5.64 Å). As this signal rapidly forms upon irradiation, it underlines our initial assignment that two different types of *Z,Z*-**A²D²** are formed from *Z*-**A**. Other species are simultaneously formed of which the signals at −120.37 and −120.68 ppm both can be assigned to **A³D³** species. The signal at −119.32 ppm could not be correlated to a macrocycle of a specific size in this measurement. However, signals between −119.2 and −119.4 ppm observed in the ^{19}F-DOSY NMR for the reaction with **D** under continuous irradiation could be assigned to species with radii between 7.02 and 7.38 Å. Judging from these values alone, this could correlate to an open macro-

cyclic species even though no signals for an aldehyde were observed in the ^{1}H NMR spectra.

Upon irradiation with UV light (405 nm), the *Z* to *E* isomerisation of the azobenzene units triggers the formation of the most stable product, which is, as previously observed, the $\mathbf{A^3D^3}$ macrocycle. Even if the MALDI-mass spectra, which were recorded during this experiment, show the formation of larger macrocyclic species up to the size of $\mathbf{A^8D^8}$ upon irradiation, this seems to take place in smaller amounts, as those species were not observed *via* NMR. To get a more detailed insight into the photoswitching of the $\mathbf{A^3D^3}$ macrocycle, we also compared its properties to those of the reduced amine $\mathbf{A^3D^3_{red}}$ (see Supporting Information, Figures S36–S42), which cannot undergo dynamic covalent exchange anymore. Preventing the dissipative formation of different macrocycles, $\mathbf{A^3D^3_{red}}$ can still be isomerised with green light, but its ability to undergo *E* to *Z* isomerisation using red light is nearly zero due to the diminished π-system. Even though $\mathbf{A^3D^3}$ is less flexible than its amine counterpart, the photoswitchability of $\mathbf{A^3D^3_{red}}$ can be an indicator that the isomerisation of $\mathbf{A^3D^3}$ could occur without opening of the macrocycle since the steric hindrance and possible ring strain do not inhibit the photoisomerisation of the azobenzenes in the macrocycle. We concluded, based on this finding, that the isomerisation of the more rigid imine compound $\mathbf{A^3D^3}$ could also be possible without breakage of imine bonds.

In conclusion, we have presented the first photoresponsive, dissipative, dynamic covalent macrocycle. By implementing visible light switchable azobenzenes into an imine macrocycle, we demonstrated a method to make dynamic covalent chemistry even more dynamic. In addition, we illustrated the diversity of structures accessible, containing metastable and highly strained systems when employing both structurally different isomers in the formation of supramolecular systems. We anticipate that our systems can contribute to the development of further out-of-equilibrium supramolecular machines and materials, where efficient control will enable the design and execution of complex novel non-covalent syntheses, resulting in a diverse range of distinct self-assembled structures based on the same building blocks.

Acknowledgements

We thank Tim Cammans for his synthetic contributions and The Center for Structural Studies, which is funded by the Deutsche Forschungsgemeinschaft (DFG Grant number 417919780) and INST 208/740-1 FUGG. B.M.S. thanks the North Rhine-Westphalian Academy of Sciences, Humanities and the Arts, and the Deutsche Forschungsgemeinschaft (DFG, German Research Foundation)—SCHM 3101/5-1 for funding. Open Access funding enabled and organized by Projekt DEAL.

Conflict of Interest

The authors declare no conflict of interest.

Data Availability Statement

The data that support the findings of this study are available in the supplementary material of this article.

Keywords: Dynamic Covalent Chemistry · Imines · Photochemistry · Self-Assembly · Supramolecular Chemistry

[1] a) T. Kunde, T. Pausch, B. M. Schmidt, *Eur. J. Org. Chem.* **2021**, 5844–5856; b) M. A. Little, A. I. Cooper, *Adv. Funct. Mater.* **2020**, *30*, 1909842; c) M. Mastalerz, *Acc. Chem. Res.* **2018**, *51*, 2411–2422; d) F. Beuerle, B. Gole, *Angew. Chem. Int. Ed.* **2018**, *57*, 4850–4878; *Angew. Chem.* **2018**, *130*, 4942–4972; e) M. Kwit, J. Grajewki, P. Skowronek, M. Zgorzelak, J. Gawroński, *Chem. Rec.* **2019**, *19*, 213–237; f) T. Hasell, A. I. Cooper, *Nat. Rev. Mater.* **2016**, *1*, 16035.

[2] a) J. Yu, D. Qi, J. Li, *Commun. Chem.* **2020**, *3*, 189; b) L. Wang, Q. Li, *Chem. Soc. Rev.* **2018**, *47*, 1044–1097; c) A. J. McConnell, C. S. Wood, P. P. Neelakandan, J. R. Nitschke, *Chem. Rev.* **2015**, *115*, 7729–7793; d) S. Yagai, T. Karatsu, A. Kitamura, *Chem. Eur. J.* **2005**, *11*, 4054–4063.

[3] a) F. A. Jerca, V. V. Jerca, R. Hoogenboom, *Nat. Chem. Rev.* **2022**, *6*, 51–69; b) Z. Zhang, W. Wang, M. O'Hagan, J. Dai, J. Zhang, H. Tian, *Angew. Chem. Int. Ed.* **2022**, *61*, e202205758; *Angew. Chem.* **2022**, *134*, e202205758; c) A.-L. Leistner, Z. L. Pianowski, *Eur. J. Org. Chem.* **2022**, *19*, e202101271; d) M. Baroncini, G. Bergamini, *Chem. Rec.* **2017**, *17*, 700–712; e) H. M. D. Bandara, S. C. Burdette, *Chem. Soc. Rev.* **2012**, *41*, 1809–1825.

[4] a) P. Lentes, E. Stadler, F. Röhricht, A. Brahms, J. Gröbner, F. D. Sönnichsen, G. Gescheidt, R. Herges, *J. Am. Chem. Soc.* **2019**, *141*, 13592–13600; b) M. Hammerich, C. Schütt, C. Stähler, P. Lentes, F. Röhricht, R. Höppner, R. Herges, *J. Am. Chem. Soc.* **2016**, *138*, 13111–13114; c) R. Siewertsen, H. Neumann, B. Buchheim-Stehn, R. Herges, C. Näther, F. Renth, F. Temps, *J. Am. Chem. Soc.* **2009**, *131*, 15594–15595.

[5] a) A.-L. Leistner, S. Kirchner, J. Karcher, T. Bantle, M. L. Schulte, P. Gödtel, C. Fengler, Z. Pianowski, *Chem. Eur. J.* **2021**, *27*, 8094–8099; b) C. Knie, M. Utecht, F. Zhao, H. Kulla, S. Kovalenko, A. M. Brouwer, P. Saalfrank, S. Hecht, D. Bléger, *Chem. Eur. J.* **2014**, *20*, 16492–16501; c) D. Bléger, J. Schwarz, A. M. Brouwer, S. Hecht, *J. Am. Chem. Soc.* **2012**, *134*, 20597–20600.

[6] a) M. Dong, A. Babalhavaeji, C. V. Collins, K. Jarrah, O. Sadovski, Q. Dai, G. A. Woolley, *J. Am. Chem. Soc.* **2017**, *139*, 13483–13486; b) S. Samanta, A. A. Beharry, O. Sadovski, T. M. McCormick, A. Babalhavaeji, V. Tropepe, G. A. Woolley, *J. Am. Chem. Soc.* **2013**, *135*, 9777–9784; c) A. A. Beharry, O. Sadovski, G. A. Woolley, *J. Am. Chem. Soc.* **2011**, *133*, 19684–1968.

[7] a) J. L. Greenfield, M. A. Gerkman, R. S. L. Gibson, G. G. D. Han, M. J. Fuchter, *J. Am. Chem. Soc.* **2021**, *143*, 15250–15257; b) M. A. Gerkman, R. S. L. Gibson, J. Calbo, Y. Shi, M. J. Fuchter, G. G. D. Han, *J. Am. Chem. Soc.* **2020**, *142*, 8688–8695; c) J. Calbo, C. E. Weston, A. J. P. White, H. S. Rzepa, J. Contreras-Garcia, M. J. Fuchter, *J. Am. Chem. Soc.* **2017**, *139*, 1261–1274; d) C. E. Weston, R. D. Richardson, P. R. Haycock, A. J. P. White, M. J. Fuchter, *J. Am. Chem. Soc.* **2014**, *136*, 11878–11881.

[8] a) M. C. Brand, N. Rankin, A. I. Cooper, R. L. Greenaway, *ChemRxiv* **2022**, https://doi.org/10.26434/chemrxiv-2022-mgwnm; b) A.-L. Leistner, D. G. Kistner, C. Fengler, Z. L. Pianowski, *RSC Adv.* **2022**, *12*, 4771–4776; c) J. Karcher, S. Kirchner, A.-L. Leistner, C. Hald, P. Geng, T. Bantle, P. Gödtel, J. Pfeifer, Z. L. Pianowski, *RSC Adv.* **2021**, *11*, 8546–8551; d) B. Moosa, L. O. Alimi, A. Shkurenko, A. Fakim, P. M. Bhatt, G. Zhang, M. Eddaoudi, N. M. Khashab, *Angew. Chem. Int. Ed.* **2020**, *59*, 21367–21371; *Angew. Chem.* **2020**, *132*, 21551–21555; e) Z. Ye, Z. Yang, L. Wang, L. Chem, Y. Cai, P. Deng, W. Feng, X. Li, L. Yuan, *Angew. Chem. Int. Ed.* **2019**, *58*, 12519–12523; *Angew. Chem.* **2019**, *131*, 12649–12653; f) A. H. Heindl, J. Becker, H. A. Wegner, *Chem. Sci.* **2019**, *10*, 7418–7425; g) E. Nieland, O. Weingart, B. M. Schmidt, *Beilstein J. Org. Chem.* **2019**, *15*, 2013–2019; h) E. Nieland, T. Topornicki, T. Kunde, B. M. Schmidt, *Chem. Commun.* **2019**, *55*, 8768–8771; i) R. Reuter, H. A. Wegner, *Chem. Commun.* **2013**, *49*, 146–148; j) T. Murase, S. Sato, M. Fujita, *Angew. Chem. Int. Ed.* **2007**, *46*, 5133–5136; *Angew. Chem.* **2007**, *119*, 5225–5228; k) L. A. Ingerman, M. L. Waters, *J. Org. Chem.* **2009**, *74*, 111–117.

[9] a) H. Lee, J. Tessarolo, D. Langbehn, A. Baksi, R. Herges, G. H. Clever, *J. Am. Chem. Soc.* **2022**, *144*, 3099–3105; b) A. D. W. Kennedy, R. G. DiNardi, L. L. Fillbrook, W. A. Donald, J. E. Beves, *Chem. Eur. J.* **2022**, *28*, e202104461; c) R. G. DiNardi, A. O. Douglas, R. Tian, J. R. Price, M. Tajik, W. A. Donald, J. E. Beves, *Angew. Chem. Int. Ed.* **2022**, *61*, e202205701; *Angew. Chem.* **2022**, *134*, e202205701; d) R.-J. Li, J. Tessarolo, H. Lee, G. H. Clever, *J. Am. Chem. Soc.* **2021**, *143*, 3865–3873; e) R.-J. Li, J. J. Holstein, W. G. Hiller, J. Andréasson, G. H. Clever, *J. Am. Chem. Soc.* **2019**, *141*, 2097–2103; f) A. D. W. Kennedy, I. Sandler, J. Andréasson, J. Ho, J. E. Beves, *Chem. Eur. J.* **2020**, *26*, 1103–1110; g) M. Han, Y. Luo, B. Damaschke, L. Gómez, X. Ribas, A. Jose, P. Peretzki, M. Seibt, G. H. Clever, *Angew. Chem. Int. Ed.* **2016**, *55*, 445–449; *Angew. Chem.* **2016**, *128*, 456–460.

[10] a) G. Ragazzon, L. Prins, *Nat. Nanotechnol.* **2018**, *13*, 882–889; b) M. Herder, J.-M. Lehn, *J. Am. Chem. Soc.* **2018**, *140*, 7647–7657; c) M. Kathan, F. Eisenreich, C. Jurissek, A. Dallmann, J. Gurke, S. Hecht, *Nat. Chem.* **2018**, *10*, 1031–1036; d) M. Kathan, P. Kovaříček, C. Jurissek, A. Senf, A. Dallmann, A. F. Thünemann, S. Hecht, *Angew. Chem. Int. Ed.* **2016**, *55*, 13882–13886; *Angew. Chem.* **2016**, *128*, 14086–14090; e) G. Ragazzon, M. Baroncini, S. Silvi, M. Venturi, A. Credi, *Nat. Nanotechnol.* **2015**, *10*, 70–75.

[11] a) M. Weißenfels, J. Gemen, R. Klajn, *Chem* **2021**, *7*, 23–27; b) B. Rieß, R. K. Grötsch, J. Boekhoven, *Chem* **2020**, *6*, 552–578; c) B. Rieß, J. Boekhoven, *ChemNanoMat* **2018**, *4*, 710–719; d) S. A. P. van Rossum, M. Tena-Solsona, J. H. van Esch, R. Eelkema, J. Boekhoven, *Chem. Soc. Rev.* **2017**, *46*, 5519–5535; e) M. Kathan, S. Hecht, *Chem. Soc. Rev.* **2017**, *46*, 5536–5550.

[12] a) V. W. L. Gunawardana, T. J. Finnegan, C. E. Ward, C. E. Moore, J. D. Badjić, *Angew. Chem. Int. Ed.* **2022**, *61*, e202207428; *Angew. Chem.* **2022**, *134*, e202207418; b) D. del Giudice, M. Valentini, G. Melchiorre, E. Spatola, S. di Stefano, *Chem. Eur. J.* **2022**, *28*, e202200685.

[13] The nomenclature introduced by Jelfs et al. labels structures as $X^m{}_pY^n$, where the two building blocks X and Y are forming one cage. X and Y can be either ditopic (Di), tritopic (Tri) or tetratopic (Tet). The superscripts m and n express the number of building blocks in each case, while p gives the number of double connections between the building blocks. For more details see: V. Santolini, M. Miklitz, E. Berardo, K. E. Jelfs, *Nanoscale* **2017**, *9*, 5280–5298.

[14] Deposition Number 2203711 (for *Z*,*Z*-$\mathbf{A^2E^2}$) contains the supplementary crystallographic data for this paper. These data are provided free of charge by the joint Cambridge Crystallographic Data Centre and Fachinformationszentrum Karlsruhe Access Structures service.

Manuscript received: August 29, 2022
Accepted manuscript online: September 27, 2022
Version of record online: October 26, 2022